JOURNAL OF SPACECRAFT AND ROCKETS
Vol. 37, No. 1, January–February 2000

# Particle Simulations of a Hall Thruster Plume

Douglas B. VanGilder,* Iain D. Boyd,† and Michael Keidar‡
*Cornell University, Ithaca, New York 14853*

**A numerical code that combines the direct simulation Monte Carlo method with the particle-in-cell method has been developed to examine the plumes of Hall thrusters. The present investigation includes a study of the sensitivity of the computed plume to various ion conditions at the thruster exit and considers models for computing the electric field based on the electron momentum equation. Specifically, two electrostatic models are compared: one assumes isothermal electrons, whereas the other uses a variable electron temperature model. Computations are compared with experimental measurements of current density, ion velocity, ion density, electron density, heat flux, and plasma potential in the plume of a stationary plasma thruster. The varying electron temperature is found to affect the very near field significantly. Simulations using this model agree better with near-field current density measurements. This model also leads to better agreement with electron number density measurements in the far field. The agreement of plasma potential depends on parameters used in the simulations. To better represent the flow inside the experimental facilities, the full chamber geometry is simulated assuming symmetry about the thruster centerline. These simulations lead to excellent agreement with current density measurements to 180 deg. The sensitivity study indicates that the far-field current density is relatively easy to reproduce.**

## Nomenclature

$E$ = electric field, V/m
$e$ = charge of an electron, C
$k$ = Boltzmann constant, J/K
$n_j$ = number density of species $j$, $m^{-3}$
$n_{ref}$ = reference electron number density, $m^{-3}$; defined where potential is 0
$p$ = pressure, $N/m^2$
$T_e$ = electron temperature, K unless specified as eV
$W_j$ = particle weight of species $j$
Xe = xenon
$\gamma$ = ratio of specific heats
$\phi$ = plasma potential, V

*Subscripts*

$e$ = electrons
$f$ = fast (high energy)
$i$ = ions
$n$ = neutrals
$r$ = radial direction
$s$ = slow (low energy)
$x$ = axial direction

*Superscript*

$+$ = ion, either singly or doubly charged

## Introduction

WITH increased commercial applications of satellites, there is a need for onboard thrusters with relatively long lifetimes. As with other electric propulsion devices, Hall thrusters offer a high specific impulse that is well suited for satellite station-keeping, repositioning, and orbit transfer. The stationary plasma thruster (SPT) variety has been used for many years. Xenon gas is currently the propellent of choice for such devices because it is an inert gas with a relatively low ionization potential. There is concern, however, about contamination of the satellite surface caused by the plasma in the plume. The charge-exchange plasma, created by collisions between ions and nonionized propellent in which electrons are transferred, is of particular concern. The charge-exchange ions have much lower velocities than the propellent ions; therefore, they are more influenced by the self-consistent electric fields. These fields may cause them to interact with spacecraft surfaces. The charged particles may impact solar arrays or interfere with transmissions from the satellite. Therefore, it is important to understand in detail the dynamics of the plume.

Computational modeling allows the dynamics of the plume and interaction with its environment to be examined without any influences of experimental facilities. The ability to simulate the plumes of these devices allows a wider variety of operating conditions to be tested than would be feasible in a laboratory. Many test chambers can be maintained at fractions of millipascals. However, the operating conditions of these devices give relatively low densities, and thus interactions between the plasma and the background gas are to be expected. Also, the walls of the chamber may influence the plasma. However, computer codes must rely on experimental data for validation. The goal of the present study is to assess the ability to simulate these plumes accurately.

To accomplish this task, a computer code that combines the direct simulation Monte Carlo[1] (DSMC) and the particle-in-cell[2] (PIC) techniques is being developed to understand in detail the plasma behavior of the plumes of Hall thrusters. The PIC method determines the trajectories of charged particles as predicted by imposed and self-consistent electric fields. The DSMC method is used to simulate the collisional effects in the flowfield. Both charge-exchange and momentum-transfer collisions are modeled. Ions and neutral atoms from the thruster and background atoms are simulated. The code has previously been verified for an ion thruster[3] and is being applied to Hall thrusters in the current study. The plumes of these two types of thrusters are similar. The main differences in modeling are in the geometry and the ratio of neutral atoms to ions. Numerical improvements to this earlier version of the code are discussed in the next section.

Because electric propulsion devices such as ion thrusters, arc jets, and Hall thrusters inherently involve charged propellent, the PIC technique is well suited to simulate their plumes. Roy[4] developed a code for modeling ion thrusters. Wang et al.[5] have also modeled ion thrusters. Previous work by Oh and Hastings[6,7] modeled SPT plumes using a PIC-DSMC code. In contrast to the work presented in Refs. 4 and 5, the neutrals are also tracked in the present study, and charge-exchange ions are generated directly from collisions

Received 8 January 1999; revision received 20 August 1999; accepted for publication 15 September 1999. Copyright © 1999 by the American Institute of Aeronautics and Astronautics, Inc. All rights reserved.

*Graduate Student, Mechanical and Aerospace Engineering. Student Member AIAA.
†Associate Professor, Mechanical and Aerospace Engineering. Senior Member AIAA.
‡Postdoctoral Research Associate, Mechanical and Aerospace Engineering.

between ions and neutrals. The underlying code (MONACO[8]) is a parallel DSMC code to which PIC routines are added. Extensive experimental data have been obtained for the SPT-100 thruster considered in the present study.[9–14] Measurements of current density and ion velocity were reported in Refs. 10 and 11. Recently, measurements of ion velocity, ion density, heat flux, neutral flux, and plasma potential were obtained.[12,13] (The reader is also referred to a private communication by C. Marrese and A. Gallimore, University of Michigan, May 1999.) The present study relies on these new data to perform the most comprehensive comparisons between experimental and computational work thus far.

The following subsections describe the assumptions and the numerical approach to the modeling, including a brief explanation of the numerical techniques used. The various simulations are described, followed by a discussion of the results and some conclusions.

## Physical Modeling

The plume is comprised of propellent ions, charge-exchange ions, neutral atoms from the thruster, electrons, and the background gas of the experimental facility. The interactions of these species as well as the influence of the electric and magnetic fields are the important modeling issues. The approach to this modeling is outlined in the following paragraphs.

Although utilization efficiencies are high for Hall thrusters, the nonionized propellent accounts for about 50% of the density at the exit. The neutral density is substantially higher when the cathode flow is included. The neutrals may undergo collisions with the ions. Many of these collisions are charge-exchange reactions, where an electron is transferred from a neutral at a relatively low velocity to a high-energy ion. The probability of such a collision is a function of relative velocity and is modeled using the cross section given by Rapp and Francis.[15] This process creates the charge-exchange ions already mentioned. At the thruster exit the nonionized propellent is modeled at sonic conditions based on a temperature of 1000 K. These assumptions yield a neutral velocity of 325 m/s, which agrees well with experiments with a similar Hall thruster.[16] The sonic assumption has been shown to lead to good agreement with experiments of neutral xenon flow.[17]

The background gas of laboratory facilities may interact with the propellent during experiments. Although the experiments considered here were conducted with a back pressure of 6 mPa, at room temperature this gives a density on the order of the thruster exit neutral density. The background gas is assumed to be composed entirely of xenon neutrals at 300 K and to be uniform. Collisions with the species that originated from the thruster are simulated, but the background particles are not tracked by the code. Instead, temporary particles are created in each cell with velocities chosen from a Maxwellian distribution and are paired for possible collisions with the species from the thruster. These may be either momentum transfer or charge-exchange reactions. At distances of more than a few centimeters from the exit plane, the background neutrals become the dominant source of charge-exchange ion production. As with the ion thruster plume considered in a previous study,[3] the changes to the neutral distribution function would be due to the fast atoms whose density would be at least three orders of magnitude lower than the bulk density. Thus, it is reasonable to assume that the background gas is unchanged with collisions, and it is unnecessary to use computational time and memory on them.

As with the previous study,[3] the ions are tracked, but the electrons are not. Instead, the electron behavior is given by a balance of the electrostatic force and the pressure gradient. Mathematically, this is

$$n_e e E = -\nabla p$$

The balance is necessary to prevent the electrons from leaving a region en masse, which would leave behind a large charge imbalance. This equation comes from the electron momentum equation and neglects the collision term and the magnetic field. For the densities and temperatures of the plasma typical of the plumes of Hall thrusters, the ion-electron collision term is negligible. The ratio of the collision frequency to the plasma frequency is much less than 1. The magnetic field term is generally neglected.[3,4,6] This appears to be a reasonable estimate for the far field. Further assuming isothermal conditions yields the familiar Boltzmann relation

$$n_e = n_{\text{ref}} \exp(e\phi / kT_e)$$

However, the near field in the plumes of Hall thrusters has variations in the electron temperature. The effects of including this variation are considered in the present study. For simplicity, the potential is not calculated in the simulations. Instead, the electric field in the axial and radial direction are calculated directly. Assuming adiabatic conditions, this becomes

$$E_{x,r} = -\frac{kT_e}{e}\frac{\mathrm{d}\ln(n_e)}{\mathrm{d}(x,r)} - \frac{k}{e}\frac{\mathrm{d}T_e}{\mathrm{d}(x,r)}$$

An electron temperature is imposed in the domain based on measurements taken by Kim et al.[15] The electrons are assumed to act as an expanding fluid at isentropic conditions. Their density decays as $r^{-2}$ and the temperature scales with $n_e^{\gamma-1}$. Constants are chosen to closely match the measurements of Kim. A comparison in Fig. 1 indicates the good agreement obtained with this approach. A far-field temperature is set for the simulations as well. Simulations are run using both models to determine the effects on the flowfield.

The difference in magnitudes of the ion and electron velocities makes it difficult to also track the electrons in the simulation. By assuming that the plasma is quasineutral ($n_i \approx n_e$), the ion density can be used to find the potential. Both singly and doubly charged propellent ions as well as the charge-exchange ions are included in the simulations. Various ion inlet conditions are used for these simulations to determine whether the comparisons with experimental data are sensitive to the ion profile at the thruster exit.

Figure 2 illustrates the computational domain used for most of the simulations. The domain is assumed to be axisymmetric about the thruster centerline. The main three-dimensional effects would come from the neutralizing cathode. The flow through the cathode is

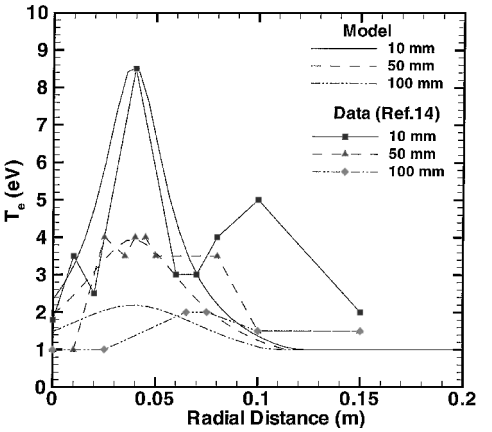


**Fig. 1 Comparison of analytical electron temperature to measurements by Kim.[14]**

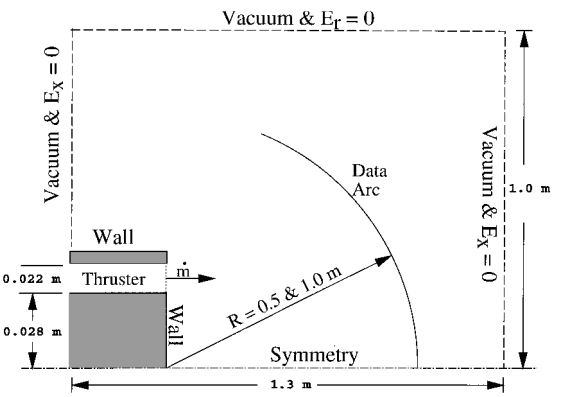


**Fig. 2 Computational domain.**

assumed to exit from the thruster as neutral xenon atoms. The radial electric field is set to zero on the centerline to satisfy symmetry, but axial variations in potential are permitted. The boundary at the maximum radial position of the domain has the same conditions. The two axial boundaries permit only radial variations in potential. For an adequately large domain the variations at the boundaries would be negligible. Particles that reach boundaries other than the symmetry line leave the simulation. The geometry below the exit plane is simplified. A wall at ground potential is assumed to extend from this exit to the centerline. When an ion strikes a wall, it is neutralized. Thus the assumption is made that an electron strikes the wall as well to maintain quasi-neutrality. The thruster wall boundary condition has little effect on the flow values compared in the results section.

Larger simulations include the full geometry of the experimental facility used at the University of Michigan as the computational domain to better represent the experimental conditions[13] in the simulations. This domain has a length of 9 m and a radius of 3 m. The walls are assumed to be at ground potential. Particles that reach the walls are removed because the background routine already maintains the facility background pressure. Again the flow is assumed to be symmetric about the thruster centerline.

## Computational Modeling

Because both the DSMC and PIC numerical methods rely on particles that represent real molecules, it is desirable to have enough particles to represent the velocity distribution adequately. The following techniques permit larger simulations than would otherwise be feasible.

The underlying DSMC code[8] is parallelized to run on the IBM SP/SP2 architecture. The computational cells are divided among the processors such that each processor maintains its own collection of neighboring cells. Parallel PIC codes also partition by blocks of cells.[18] However, in the present implementation separate grids are maintained by the two algorithms. The data structures are defined such that the particles are associated with the DSMC grid. These particles are then implicitly mapped to the PIC nodes. For these reasons the PIC algorithm can be run in parallel by a simple tree sum of the charge density at the nodes. The overhead in this method is that each processor has a copy of the entire PIC grid and must calculate the electric field for the entire domain. However, these physical models only require a central differencing scheme for calculating the electric field. By making this simple change to the PIC part of the code, advantage is taken of the underlying parallelization of the DSMC code. For completeness, one time step of the algorithm is shown in Fig. 3.

The behavior of the ions is of primary interest. A sufficient number of ion particles are needed in each cell to represent the ion density for the PIC method without introducing artificial gradients. Therefore, to increase the ion particle count without creating an overabundance of neutrals, a particle weighting scheme is used. The method outlined by Bird for species weighting only conserves momentum and energy on the average, not in each collision.[1] This approach is not conducive to flows with few collisions. A method developed by Boyd[19] splits the particle with the larger weight into two parts. One of these has its momentum changed according to the collision dynamics, and the two parts are recombined afterwards. However, for collision pairs with vastly different velocities, this technique fails to represent the velocity distribution of the species with the larger weight. Charge-exchange reactions commonly involve collision pairs of this type. For this reason a new particle weighting scheme is used for the charge-exchange reactions, whereas Boyd's scheme is used for momentum transfer.

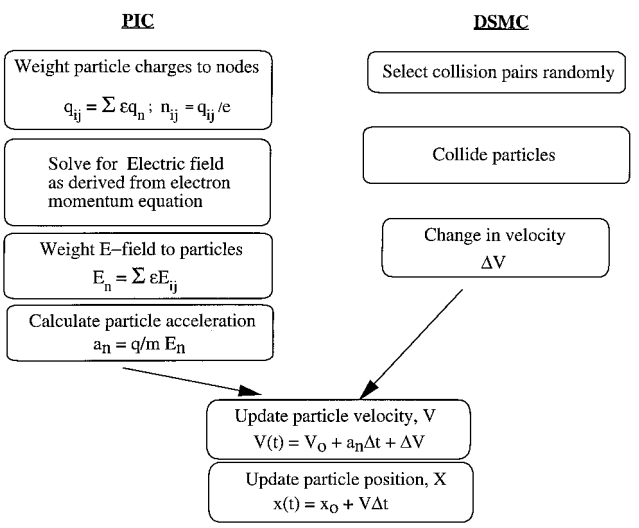


**Fig. 3 One time step of the DSMC-PIC algorithm.**

The present scheme is generalized for ion-neutral collisions regardless of which particle has the larger weight, but in these cases the neutral either has an equal or larger weight. The reaction can be described by the following equation:

$$W_n Xe_s + W_i Xe_f^+ \rightarrow (W_n - W_i)Xe_s + W_i Xe_f + W_i Xe_s^+$$

This scheme has the drawback that a third particle is created in each charge-exchange reaction. However, the mean free path is large enough ($\approx 1.2$ m at the thruster exit) that this is not a concern. Physically, this shows that only $W_i$ of the $W_n$ molecules undergo a collision and the others are unchanged. This leaves a distribution of $W_n - W_i$ molecules at the same velocity and the other $W_i$ with a much higher velocity. If these two particles were instead recombined using Boyd's scheme, $W_n$ molecules would have a velocity between the extremes that none of these molecules physically would have.

Most of the simulations employ 700,000–800,000 particles in 1600 DSMC cells and 9500 PIC cells on an IBM SP2. These simulations require about 50 CPU h distributed over four processors because the charge-exchange ion timescale is large compared to the propellent ions. Parallel efficiency ranged from 80 to 90%. The fluctuations are caused by the particle weighting scheme. Periodically, a load-balancing routine is used to distribute the particles more evenly among the processors.

## Flow Conditions

The nominal operating conditions given in the experiments considered are a current of 4.5 A, a discharge voltage of 300 V, a total flow rate of 5.2–5.4 mg/s with 7% cathode split, and a facility backpressure of 6 mPa. An ion temperature of 4 eV is assumed at the exit based on Ref. 11 for most of the cases and is compared with a 0.4 eV case (labeled case 3 in the figures). The electron temperature is assumed to be 3 eV based on Ref. 9 and is used to obtain the potential from the Boltzmann relation. These parameters define the input values, but it is necessary to separate them into densities and velocities for each species. The fraction of doubly charged ions is estimated as 25% by Manzella and Sankovic[10] for an SPT-100. This value along with the thruster's efficiency and the assumptions about the neutrals allows exit plane properties for each species to be determined.

The efficiency obtainable at nominal conditions is approximately 0.5 for the SPT-100 Hall thruster.[20] A value of 0.54 is chosen for this investigation, which gives an ion velocity close to King's measurements.[12,13] The ions leave the thruster with a radial component to their velocity.[11] Oh and Hastings inverted an analytic function to choose a divergence angle for each particle.[7] The present study simplifies this process by assuming the divergence angle varies linearly with radial distance from the center of the annulus ring. A maximum of 10 deg is used in one case and 20 deg in another. A uniform ion velocity (0 m/s radial velocity) case is also considered for comparison with current density and heat flux measurements. Each generated ion is chosen from a Maxwellian distribution with the specified average velocity. These velocity profiles are combined with a uniform ion density. See Table 1 for a list of thruster exit conditions used for the sensitivity study.

Table 2 shows the input conditions for examining the effects of a varying electron temperature. The main difference from the other input conditions is that these cases have only 10% of the propellent ions assumed to be doubly charged,[13] but this negligibly affects

**Table 1 Ion conditions at thruster exit for sensitivity study**

| Case | Speed, km/s | Velocity variation | Temperature, eV |
|---|---|---|---|
| 1 | 17.6 | $f(r)$: 10 deg | 4 |
| 2 | 17.8 | $f(r)$: 20 deg | 4 |
| 3 | 17.6 | $f(r)$: 10 deg | 0.4 |
| 4 | 17.5 | Uniform | 4 |

**Table 2 Input conditions for modeling study**

| Case | $T_e$, eV | $T_e$ profile | $n_{e\infty}$, $m^{-3}$ |
|---|---|---|---|
| Ref* | 3.0 | Constant | 6.5*e*15 |
| VT 1 | 1.0 | Varying | 6.5*e*15 |
| VT 2 | 2.0 | Varying | 6.5*e*15 |
| VT 3* | 2.0 | Varying | 1.3*e*15 |

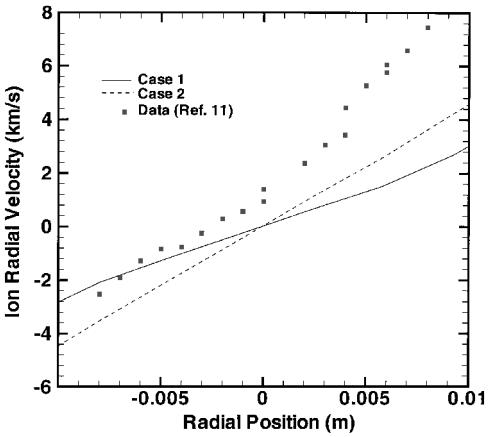


**Fig. 4 Comparisons of ion radial velocity at an axial distance of 11 mm.**

aggregate ion properties in the plume. The value for reference electron number density determines the magnitude of the potential, but has little effect on the differences in the potential. The value of the electron temperature for the variable electron temperature cases represents the far-field value imposed. The cases marked with asterisks include a full chamber geometry simulation as well as a smaller domain one.

## Results

Measurements of radial velocity by Manzella[11] indicate an almost linear variation with radial position 11 mm from the thruster exit. A comparison of the simulations with this data is shown in Fig. 4. The simulations also give an almost linear variation that is reasonably close to the data at this axial location. There are significant discrepancies between simulation and data. Neither case reproduces the asymmetry found experimentally because it was not included in the thruster exit plane profile for this investigation.

Comparisons of current density for various simulations with experiments are presented at two different radial locations in Figs. 5–7. The base case (case 1) shown in Fig. 5 agrees well with King's experiment.[12] The comparisons in Figs. 6 and 7 indicate the insensitivity of the computed current density to the variations in inlet ion profiles. The variations are more pronounced close to the centerline; however, each case is within a factor of about two of the data. Comparing cases 1, 2, and 4 indicates the significance of the divergence angle. Clearly, the higher angle leads to a lower peak value at these radial distances. Experiments show a more defined peak than the simulations. The low ion temperature case (case 3) gives a more defined peak, but an underprediction of current density occurs at higher angles.

In Figs. 8–10 the current density is separated into density and velocity components. The velocity comparisons in Figs. 8 and 9 indicate agreement within experimental uncertainty up to about 50 deg. The simulation results only present the average ion velocity

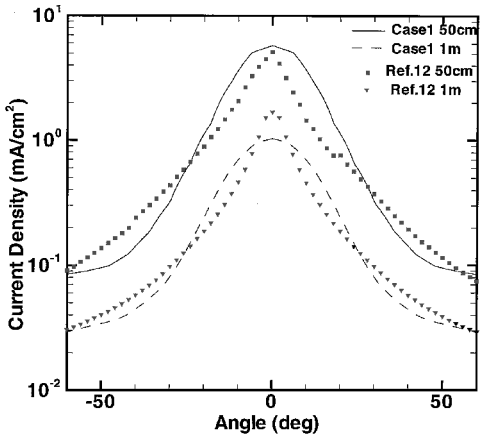


**Fig. 5 Comparisons of current density at radial distances of 50 cm and 1 m.**

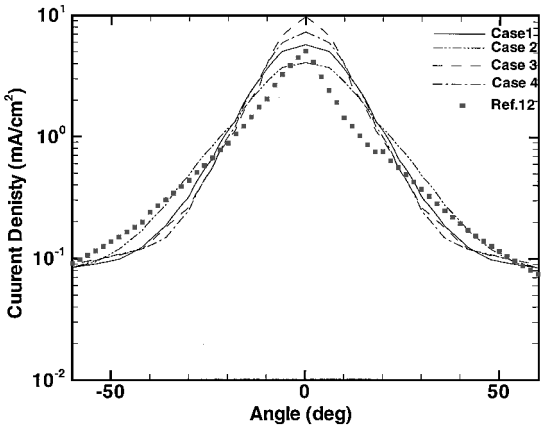


**Fig. 6 Comparisons of current density at a radial distance of 50 cm.**

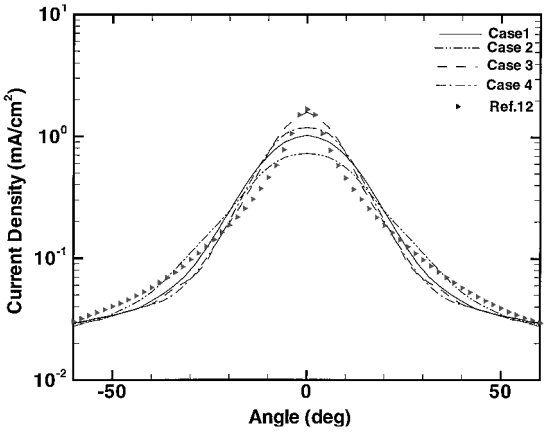


**Fig. 7 Comparisons of current density at a radial distance of 1 m.**

of the propellent ions, neglecting the charge-exchange ions. The experimental data were obtained from a retarding potential analyzer (RPA).[13] Numerical differentiation of the current vs voltage data approximates the derivative of this curve, which is proportional to the energy-per-charge distribution function. For singly charged ions of uniform mass, the energy distribution function also represents the velocity distribution function. By normalizing and numerically integrating this velocity distribution function, the average velocity is obtained. This process is likely to minimize the effects of the charge-exchange ions because they only contribute to the current measurements at low voltages. Also, the current scales with the flux of the charge-exchange ions. Thus, the density that is needed to obtain the actual contribution of the charge-exchange ions to the average velocity may be obscured. Therefore, comparing the average

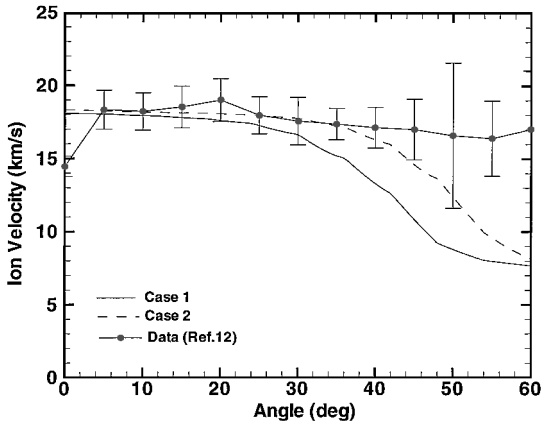


**Fig. 8 Comparisons of average ion velocity at a radial distance of 50 cm.**

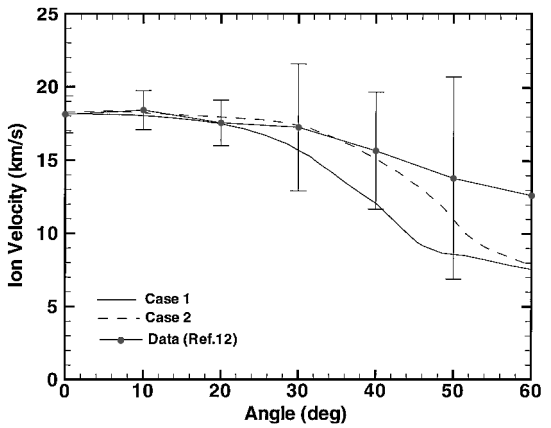


**Fig. 9 Comparisons of average ion velocity at a radial distance of 1 m.**

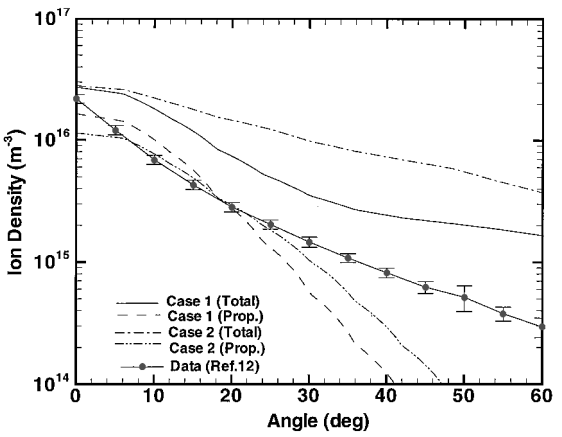


**Fig. 10 Comparisons of ion density at a radial distance of 50 cm.**

ion velocity of only the propellent ions from the simulation with the experimental measurements is reasonable. The agreement is encouraging. The ion velocity and current density are used to obtain the experimental number density shown in Fig. 10. The simulations allow the ion density to be given directly. Both total density and the propellent ion density of the simulations are shown in Fig. 10. The propellent ion density agrees well at low angles, but it is too low at higher angles where the charge-exchange ions represent a higher fraction. The profile of the total density for case 1 compares favorably with the experiment, but the magnitude is too high. Following the same reasoning as described earlier, the measured ion density should be between the total and propellent densities from the simulation. In contrast to the ion velocity comparisons in Figs. 8 and 9, case 2 does not represent the ion density as well as case 1.

Heat flux measurements were obtained by a heat flux probe consisting of two Schmidt–Boelter thermophile transducers.[13] The probe was biased to ground potential, which was between 5 and 8 V below the plasma potential, to eliminate electron current heating. Thus, the measured heat flux includes both neutrals and ions. The simulations give the contributions of the ions and the propellent neutrals. The background neutrals contribution is negligible. It is estimated to be on the order of 1 W/m$^2$. In Figs. 11–13 comparisons of the simulations with heat flux measurements are shown. There is agreement near the thruster centerline at 50 cm. At 1 m the simulated heat flux is within a factor of three of the measurements. At large angles from the centerline, where charge-exchange ions dominate, there is an underprediction by two orders of magnitude at both locations. The charge-exchange ions have much lower velocities than the propellent ions, and the heat flux scales with velocity

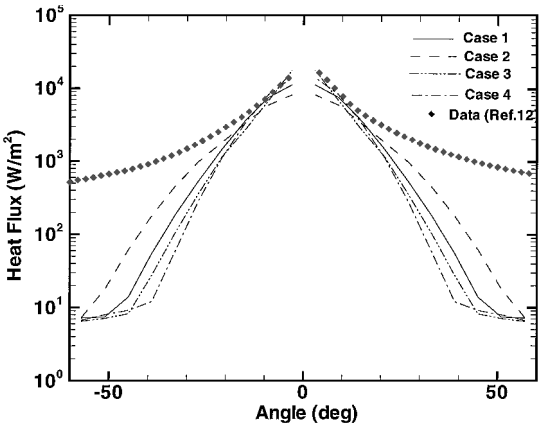


**Fig. 11 Comparisons of heat flux at a radial distance of 50 cm.**

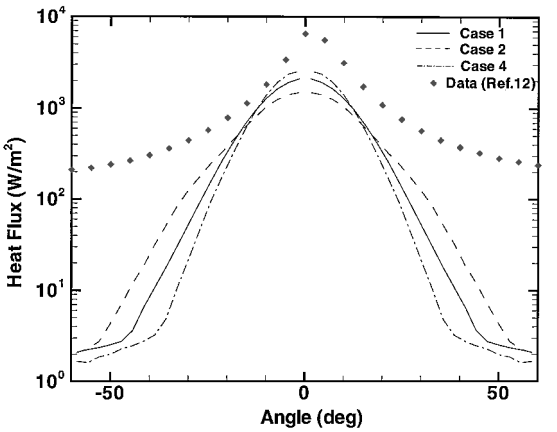


**Fig. 12 Comparisons of heat flux at a radial distance of 1 m.**

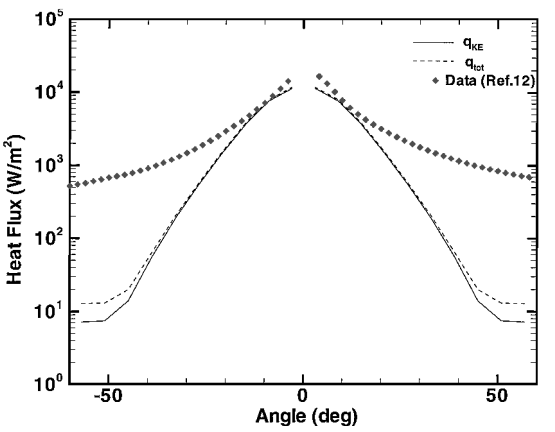


**Fig. 13 Comparisons of total heat flux at a radial distance of 50 cm.**

**Table 3 Integrated heat flux at various radial locations**

| Case | 50 cm, W | 1 m, W |
|---|---|---|
| King | 1692 | 2339 |
| 1 | 630.0 | 449.4 |
| 2 | 637.8 | 460.0 |
| 3 | 609.6 | 410.1 |
| 4 | 618.3 | 424.8 |
| Ref | 652.5 | 454.9 |
| VT 1 | 678.0 | 468.6 |
| VT 2 | 678.5 | 472.6 |
| FG VT | 680.3 | 478.3 |

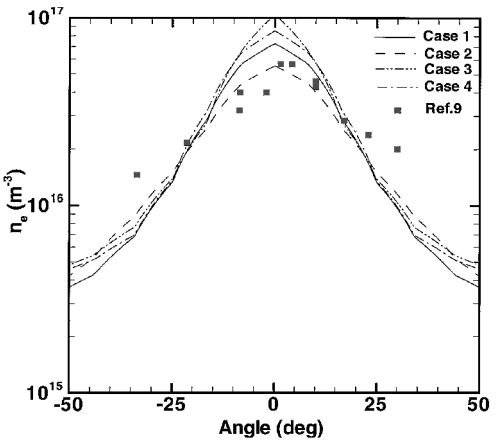


**Fig. 14 Comparisons of electron density with measurements by Myers[9] at a radial distance of 31 cm.**

cubed. The spreading of the propellent ions does not improve the agreement at the higher angles significantly, and it leads to poorer agreement near the centerline (Figs. 11 and 12). As with the ion density comparisons, a divergence angle ranging from −20 to 20 deg does not lead to as good agreement as the other cases. The ion temperature has a surprisingly small effect on the heat flux (Fig. 11). The ion temperature affects the spreading of the beam without altering the magnitude of the mean velocity. The higher temperature allows more spreading. The heat flux at higher angles should increase with ion temperature because its magnitude varies as velocity cubed. To estimate the effect on the ions of biasing the probe, an energy of 8 eV is added per ion to the heat flux calculations and is labeled $q_{\text{tot}}$ in Fig. 13. Clearly, it is only significant at the larger angles, but it does not make a substantial difference. Upon integrating the heat flux from the experiments, it is found that this heat transfer rate is greater than the power put into the system. Integrated values for the heat flux are shown in Table 3. The electrical power is only 1350 W. The simulations give values indicative of the measured efficiencies (≈50%) at a radial distance of 50 cm. By 1 m collisions with the background neutrals have decreased the energy of the ion flow. The simulations, which include a varying electron temperature model, are also included in the table, but plots of the heat flux show only moderate differences from the reference case.

Calculated values for electron density are compared with measurements by Myers and Manzella[9] at a radial distance of 31 cm in Fig. 14. Cases 1 and 2 show the best agreement. The other cases have inlet conditions that lead to less spreading of the ions. The electron densities from the other set of test cases are shown in Fig. 15. Including a varying electron temperature affects the spreading of the ions. The radial electric field is larger than it would be without a temperature gradient. The case labeled "Ref" is nearly identical to case 1. It is clear from Fig. 15 that the case labeled "VT 3" agrees best with the measurements.

Comparisons with measurements of current density in the plume near field by Kim[14] are shown in Figs. 16 and 17 at three axial locations. At an axial distance of 10 mm, the agreement is reasonable regardless of varying the electron temperature. However, by 100 mm the effects of this temperature gradient are more apparent. The ion

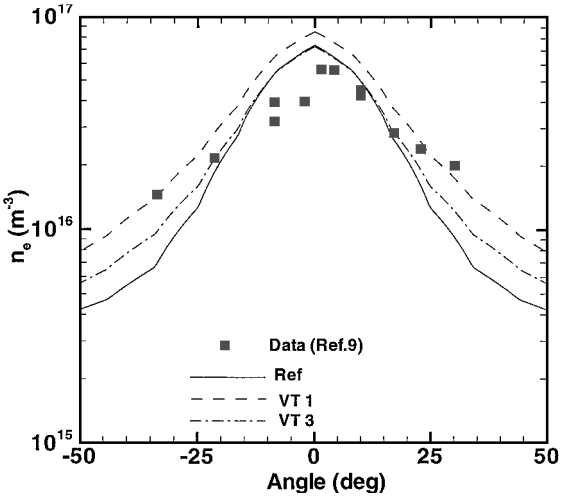


**Fig. 15 Comparisons of electron density with measurements by Myers[9] at a radial distance of 31 cm.**

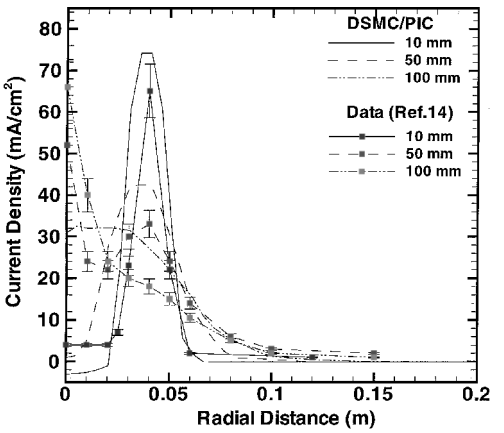


**Fig. 16 Comparisons of current density from reference case with measurements by Kim.[14]**

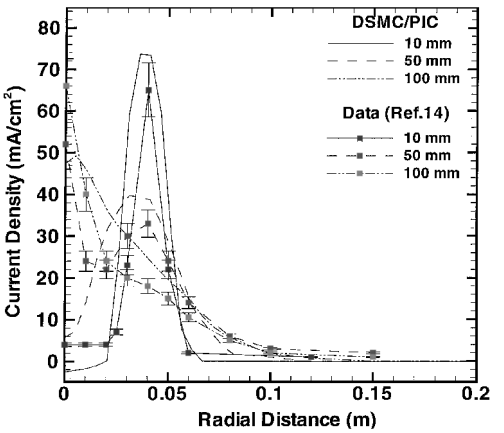


**Fig. 17 Comparisons of current density from variable electron temperature case with measurements by Kim.[14]**

beam reaches the axis more quickly than is predicted by the reference case. The variable electron temperature case more closely matches the shape of the measurements at 100 mm than the reference case. Its peak is about 50% higher than that of the reference case. Even by 50 mm the current density is higher at the axis for a varying electron temperature. For these near-field comparisons there is negligible difference between the different variable electron temperature cases; therefore, only the first is shown. Integrated values are compared in Table 4. At 10 and 100 mm, varying the electron temperature gives only a 4% difference in integrated current.

**Table 4 Integrated current at various axial locations**

| Case | 10 mm | 25 mm | 50 mm | 100 mm |
|---|---|---|---|---|
| Kim | 3.97 A | 4.92 A | 4.95 A | 4.51 A |
| Ref | 4.04 A | —— | 4.09 A | 4.19 A |
| VT 1 | 4.14 A | —— | 4.24 A | 4.33 A |
| VT 3 | 4.13 A | —— | 4.22 A | 4.32 A |

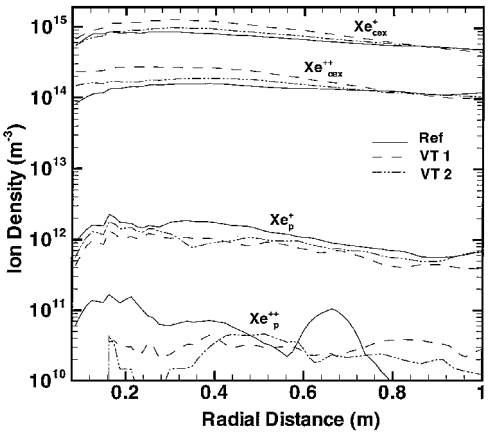


**Fig. 18 Comparisons of ion density for the various simulations at an axial distance 4 cm behind the thruster.**

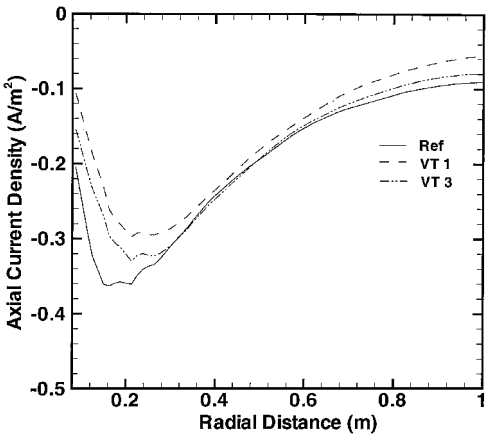


**Fig. 19 Comparisons of axial current density for the various simulations at an axial distance 4 cm behind the thruster.**

For contamination concerns the backflow and far-field regions are more significant than the near field. The next few figures compare the reference case with the variable electron temperature cases. Figure 18 shows the densities of the various ions 4 cm behind the thruster. Clearly, the charge-exchange ions are most dominant. This is also true well above the thruster in the radial direction because the propellent ions are predominantly axially directed. Comparisons of the charge-exchange ions both behind the thruster and above it for the various cases indicate the significance of the magnitude of the far-field electron temperature. More importantly, the current density shows differences at these locations (Figs. 19 and 20). Behind the thruster the reference case has a magnitude that is a factor of two higher than the $T_e = 1$ eV case near the thruster and 50% higher near the top of the domain. The results are similar at 70 cm above the thruster as well in both the axial and radial directions.

Simulations, which include the full vacuum chamber geometry, allow comparison with experimental data at large angles in the backflow region. The current density from the full geometry cases are compared with measurements by King[13] at a radius of 50 cm and 1 m in Fig. 21. Even at large angles behind the thruster, good agreement is obtained for both models. The relative insensitivity of the current density to the varying electron temperature coupled with the differences in electron number density suggests that the far-field electron temperature is important.

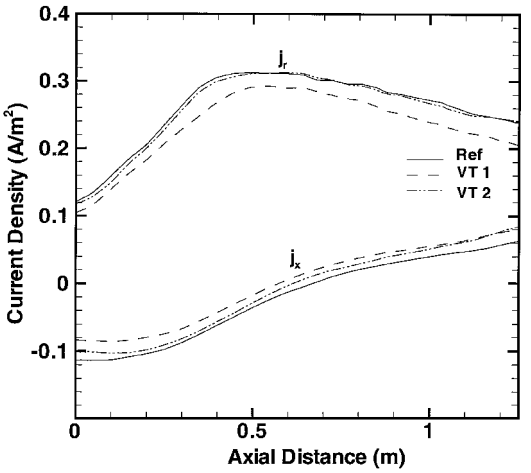


**Fig. 20 Comparisons of current density for the various simulations at a radial distance 0.7 m above the thruster.**

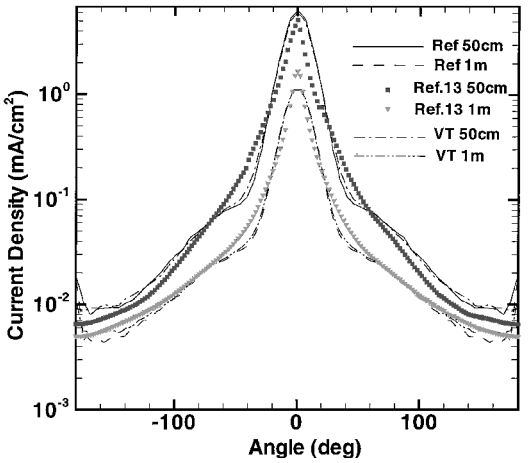


**Fig. 21 Comparisons of current density with measurements by King.[13]**

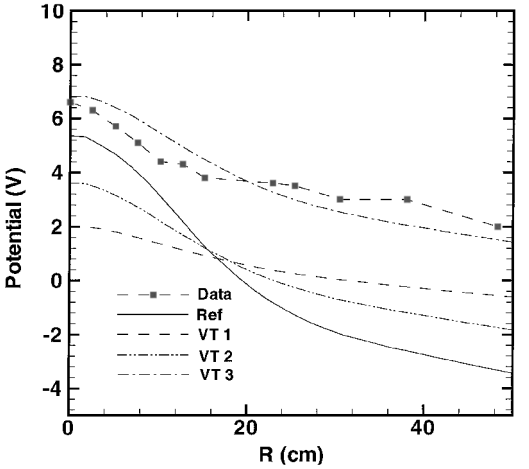


**Fig. 22 Comparisons of potential with measurements by Marrese (from private communication with A. Gallimore) at an axial distance of 48 cm.**

The plasma potential is compared with measurements taken by Marrese and Gallimore (C. Marrese and A. Gallimore, University of Michigan, May 1999, private communication) at an axial distance of 48 cm in Fig. 22. In the simulations the potential drops below zero because of the choice of the reference electron density used in inverting the Boltzmann relation. The experimental measurements here and by King and Gallimore[13] (in Fig. 23) do not become negative. The third variable electron temperature simulation is shown, which uses a lower value for the reference number density based on Marrese's measurements. This value also agrees with the far-field

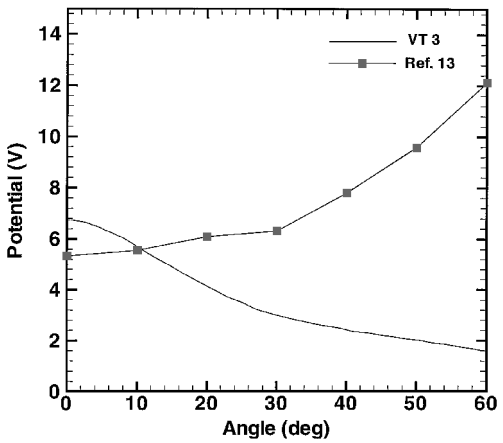


**Fig. 23 Comparisons of plasma potential with measurements by King[13] at a radial distance of 50 cm.**

electron density of the simulations. This simulation matches Marrese's data well. The first two variable electron temperature cases have the same shape as Marrese's data but are negative like the reference case. The agreement with King's data (in Fig. 23) is less encouraging. The shape of the potential profile measured experimentally is explained in Ref. 21 through a detailed analysis of the effect on plasma potential of the magnetic configuration of several different Hall thrusters.

## Conclusions

A computer code has been developed for simulating Hall thruster plumes. In this study the focus was on examining the sensitivity of the flowfield to various ion inlet conditions as well as to different models for computing the electric fields based on the electron momentum equation. Simulations were performed for the SPT-100 at nominal operating conditions, and comparisons with measured data were presented for a number of plume properties including current density in the near-field, far-field, and backflow regions, and for electron density, heat flux, and plasma potential.

Numerical issues such as computational time and memory cause restraints on the ability to perform large-scale simulations. A particle weighting scheme was used to allow a sufficient number of ions in the computational domain without an overabundance of neutral particles. This scheme better represents the velocity distribution than a weight-by-species method. The parallel nature of the code allows large-scale simulations. These two numerical techniques offer the capabilities of accurately simulating the physical models.

Calculations of far-field ion properties are affected by variations in the ion inlet profile. However, the comparisons with experimental data show only moderate differences. Each of the various simulations agreed well with experimental measurements of far-field ion current density.

Including a varying electron temperature was found to be significant in the modeling of Hall thruster plumes. The electron temperature gradient significantly affects the near-field of the plume. Simulations incorporating the varying electron temperature model gave better agreement with the near-field current density measurements than those using the isothermal Boltzmann relation. Results suggest that outside of this region the plasma behavior is not dictated by this near-field behavior, but rather by the value of the electron temperature. Thus, the far-field electron temperature is also important. This temperature is likely to be lower than the near-field value. The simulations agreed well with the measurements of electron number density. Agreement with plasma potential was dependent on the value for the reference density used in the physical models.

Simulating the full geometry of the experimental facility is important to consider measurements for code validation of the backflow region. This can also aid in determining any possible effects from the facility. The simulations were found to represent the current density very well. Even at large angles behind the thruster, good agreement was obtained with experiment.

## Acknowledgments

Funding for this research was provided by NASA John H. Glenn Research Center through Grant NAG3-1451 and by the Air Force Office of Scientific Research through Grant F49620-96-1-0091. The authors also wish to thank Lyon B. King for making the experimental data available for comparison.

## References

[1]Bird, G. A., *Molecular Gas Dynamics and the Direct Simulation of Gas Flows*, Oxford Univ. Press, Oxford, 1994.

[2]Birdsall, C. K., and Langdon, A. B., *Plasma Physics via Computer Simulation*, Adam Hilger, Bristol, England, U.K., 1991.

[3]VanGilder, D. B., Font, G. I., and Boyd, I. D., "Hybrid Monte Carlo–Particle-in-Cell Simulation of an Ion Thruster Plume," *Journal of Propulsion and Power*, Vol. 15, No. 4, 1999, pp. 530–538.

[4]Roy, R., Samanta, "Numerical Simulation of Ion Thruster Plume Backflow for Spacecraft Contamination Assessment," Ph.D. Dissertation, Dept. of Aeronautics and Astronautics, Massachusetts Inst. of Technology, Cambridge, MA, May 1995.

[5]Wang, J., Brophy, J., and Brinza, D., "3-D Simulations of NSTAR Ion Thruster Plasma Environment," AIAA Paper 96-3202, July 1996.

[6]Oh, D., and Hastings, D., "Three Dimensional PIC-DSMC Simulations of Hall Thruster Plumes and Analysis for Realistic Spacecraft Configurations," AIAA Paper 96-3299, July 1996.

[7]Oh, D., and Hastings, D., "Axisymmetric PIC-DSMC Simulations of SPT Plumes," International Electric Propulsion Conf., Paper 95-160, Sept. 1995.

[8]Dietrich, S., and Boyd, I. D., "Scalar and Parallel Optimized Implementation of the Direct Simulation Monte Carlo Method," *Journal of Computational Physics*, Vol. 126, 1996, pp. 228–243.

[9]Myers, R. M., and Manzella, D. H., "Stationary Plasma Thruster Plume Characteristics," International Electric Propulsion Conf., Paper 93-096, July 1993.

[10]Manzella, D. H., and Sankovic, J. M., "Hall Thruster Ion Beam Characterization," AIAA Paper 95-2927, July 1995.

[11]Manzella, D. H., "Stationary Plasma Thruster Ion Velocity Distribution," AIAA Paper 94-3141, Aug. 1994.

[12]King, L. B., and Gallimore, A. D., "Ionic and Neutral Particle Transport Property Measurements in the Plume of an SPT-100," AIAA Paper 96-2712, July 1996.

[13]King, L. B., "Transport-Property and Mass Spectral Measurements in the Plasma Exhaust Plume of a Hall-Effect Space Propulsion System," Ph.D. Dissertation, Dept. of Aerospace Engineering, Univ. of Michigan, Ann Arbor, MI, May 1998.

[14]Kim, S., Foster, J. E., and Gallimore, A. D., "Very-Near-Field Plume Study of a 1.35 kW SPT-100," AIAA Paper 96-2972, July 1996.

[15]Rapp, D., and Francis, W. E., "Charge Exchange Between Gaseous Ions and Atoms," *Journal of Chemical Physics*, Vol. 37, No. 11, 1962, pp. 2631–2645.

[16]Cedolin, R. J., Hargus, W. A., Jr., Hanson, R. K., and Capelli, M. A., "Laser-Induced Fluorescence Diagnostics for Xenon Hall Thrusters," AIAA Paper 96-2986, July 1996.

[17]Boyd, I. D., VanGilder, D. B., and Liu, X., "Monte Carlo Simulation of Neutral Xenon Flows of Electric Propulsion Devices," *Journal of Propulsion and Power*, Vol. 14, No. 6, 1998, pp. 1009–1015.

[18]Roy, R., Samanta, Hastings, D. E., and Taylor, S., "Three-Dimensional Plasma Particle-in-Cell Calculations of Ion Thruster Backflow Contamination," *Journal of Computational Physics*, Vol. 128, 1996, pp. 6–18.

[19]Boyd, I. D., "Conservative Species Weighting Scheme for the Direct Simulation Monte Carlo Method," *Journal of Thermophysics and Heat Transfer*, Vol. 10, No. 4, 1996, pp. 579–585.

[20]Sankovic, J. M., Hamley, J. A., and Haag, T. W., "Performance Evaluation of the Russian SPT-100 Thruster at NASA LeRC," International Electric Propulsion Conf., Paper 93-094, Sept. 1993.

[21]Keidar, M., and Boyd, I. D., "Effects of a Magnetic Field on the Plasma Plume from Hall Thrusters," *Journal of Applied Physics*, Vol. 86, No. 9, 1999, pp. 4786–4791.

R. G. Wilmoth
*Associate Editor*